

2 Diagnosis of spinal tuberculosis

J. Naresh-Babu

Introduction

The successful management of spinal tuberculosis (TB) depends on early diagnosis and early initiation of chemotherapy. Spinal TB, which is the commonest form of extra-pulmonary TB, typically presents late. Delayed diagnosis is often attributed to diseases mimicking spinal TB. The diagnosis of spinal TB is often difficult due to pauci-bacillary nature of the disease. A combination of high clinical suspicion, proper radiological imaging, and histopathological and molecular methods is needed for prompt diagnosis.

This chapter discusses the various clinical presentations, characteristic radiological features, and different clinical presentations of spinal TB of various locations. This chapter also highlights various conditions mimicking spinal TB and their differentiating features.

Clinical diagnosis

The classical presenting symptoms of TB spondylodiskitis include pain associated with constitutional symptoms, deformity, cold abscesses, and related neurological symptoms. Clinical presentation can be extremely variable with nonspecific and insidious onset of symptoms leading to delay in diagnosis.

General symptomatic presentation

The presenting symptoms depend upon the severity and duration of the disease, region of involvement, and associated complications. Gait and posture of the patient vary depending on the affected segment. In cervical

spine lesions, the patient can have torticollis with neck supported by hand, military gait with stiff upper back in upper thoracic spine involvement, and Alderman's gait with hyperlordosis in lower thoracic and lumbar spinal involvement (**Table 2.1**).

Axial pain is noticed in 90–100% of patients and is attributed to chronic inflammation, instability, and pressure from abscess. Constitutional symptoms like fever, malaise, loss of appetite, and fatigue are commonly associated with spinal TB. Paravertebral swelling without any signs of inflammation is present in almost 50% of cases, either in superficial or deeper planes and track along paths of least resistance into various planes like perineural, perivascular, intramuscular, subpleural, and retroperitoneal regions.

Complete destruction of one vertebral body results in about 30° of kyphosis. It may present as knuckle, gibbus, or rounded type based on number of vertebral segments involved¹ (**Fig. 2.1**). Skip lesions and multiple segment involvement are common in tubercular spine.²



Fig. 2.1 Clinical pictures showing severe kyphotic deformity due to involvement of a large number of thoracic vertebrae.

Table 2.1 Clinical features of TB spondylodiskitis specific to the region of involvement

Location	Clinical features	Clinical significance
Craniovertebral junction	Dysphagia, painful torticollis, neurological deficit can range from monoparesis to quadriparesis	Rare, can be life threatening
Cervical spine	Neck pain, rigidity, brachialgia, torticollis, dysphagia, hoarseness of voice, respiratory stridor	Less common, potentially morbid
Cervicothoracic junction (C7–T3)	Kyphosis, large abscess, progressive neurological deficits	Junctional disease, can lead to spinal instability
Thoracic spine	Swelling in the chest wall/mediastinum manifesting as radiating pain to chest, abdomen, or girdle region	Most common involvement, cold abscess presents as fusiform paravertebral swelling, potential for neurological deficits
Thoraco-lumbar junction (T10–L2)	Severe kyphotic deformity, instability and progressing neurological symptoms	Junctional disease leading to spinal instability
Lumbar spine	Back pain often associated with radiculopathy, stiffness, restricted movements with minimal deformity	Swellings due to cold abscess in Petit's triangle, groin, Scarpa's triangle, and gluteal region
Lumbo-sacral junction	Cauda-equina compression but with weak or absent reflexes	Junctional disease leading to spinal instability

Abbreviation: TB, tuberculosis.

Neurological deficits can be either early-onset type (within first 2 years) or late-onset type (healed stage). The incidence is around 10–20% in highly developed countries and 20–41% in developing nations.³ Direct compression due to abscess, inflammatory tissue, sequestrum, or instability is the usual cause for neural compromise in the active stage. Late-onset type of deficits are due to exaggerated movements, mechanical stretch of cord over an internal gibbus, or ossified ligamentum flavum proximal to deformity rarely.⁴ Patients initially present with weakness of legs, altered gait, exaggerated reflexes, and extensor plantar response due to involvement of anterior and lateral tracts. Eventually posterior column gets affected resulting in loss of sensation, and bowel and bladder dysfunction.⁵

Symptomatology is based on specific regional involvement of the spine

Craniovertebral junction TB is a rare entity but with life-threatening sequelae. Abscesses or granuloma formed secondary to the disease may cause compression of the upper cervical cord and bulbo-medullary complex

leading to different complications like painful torticollis, dysphagia, mono/hemiparesis to tetraparesis.

Cervical spine TB is a less common presentation but can be potentially morbid due to severe neurologic complications. Common complaints are neck pain associated with rigidity, brachialgia, and torticollis. Cold abscess in retropharyngeal space can manifest as dysphagia, hoarseness of voice, and respiratory stridor, or track along the brachial plexus to axilla region.^{6,7}

Cervicothoracic junction (C7–T3) being the transitional zone between lordotic cervical and kyphotic thoracic spine, involvement of this zone causes spinal instability, severe kyphosis, large abscesses, and progressive neurological deficits.

Thoracic spine is the most common site of involvement usually with fusiform paravertebral swelling which tracks along intercostal neurovascular bundles, presenting as swelling in the chest wall/mediastinum and manifesting as radiating pain to chest, abdomen, or girdle region, or may track down through the arcuate ligament to form lumbar abscess. Paraplegia commonly occurs in this region.⁸

Throacolumbar junction (T10-L2) is transitional area between relatively fixed, kyphotic thoracic spine and mobile lordotic lumbar spine. Destruction in this region leads to severe kyphotic deformity, instability, and progressing neurological symptoms.

Lumbar spine usually presents with back pain often associated with radiculopathy, stiffness, restricted movements with minimal deformity, and swellings due to cold abscess present within the Petit's triangle or in the groin and can track down along the psoas muscle leading to pseudo-flexion deformity of hip joint. Rarely it can track along the femoral or gluteal vessels to present as swellings in the Scarpa's triangle or gluteal region.^{9,10}

Lumbo-sacral junctional biomechanics, influenced by the natural lumbar lordosis, influence the pattern and progression of deformity. The cold abscess can track down along the iliopsoas and presacral regions. Cauda-equina compression due to lumbar and sacral vertebral damage causes weakness, numbness, and pain, but results in decreased or absent reflexes among the affected muscle groups in contrast to hyperreflexia seen with spinal cord compression along with bladder involvement (cauda-equina syndrome).

Radiological diagnosis of tuberculous spondylodiskitis

Introduction and overview

Conventional radiographs help in identifying narrowed intervertebral disk spaces and providing an overview of

the spinal deformity, but disko-vertebral lesions, spinal canal dimensions, and paravertebral abscess are better visualized on magnetic resonance imaging (MRI) and computed tomography (CT).¹¹ Hence, the importance of CT, MRI, and positron emission tomography-computed tomography (PET-CT) scans is being highlighted due to increase in their accuracy to pick up the disease at an early stage.

Plain radiography and CT scan

Plain orthogonal radiographs are the first imaging studies in any case of chronic back pain irrespective of etiology. Corresponding to the pathophysiology, the radiographic changes initially appear in the anterior margin of the vertebral body adjacent to the end plates followed by adjacent intervertebral disk destruction¹² (**Fig. 2.2a**).

To appreciate osteolysis on plain radiographs, at least one-third of the calcium content has to be lost; hence, many changes may be unnoticed until there is marked vertebral body and disk destruction.¹⁵ The earliest changes noted are vertebral body osteoporosis, obliteration of the intervertebral disk space, para-diskal haziness, end plate erosions (**Fig. 2.2b, c**), and paravertebral soft tissue shadows² (**Fig. 2.2d-g**). With the progression of disease, extensive vertebral destruction causes collapse resulting in asymmetric wedging or kyphosis. In advanced disease, collapse of the vertebrae gives rise to a radio-dense fusiform and globular shadow, "bird nest" appearance (**Fig. 2.3**). Lateral translation of the vertebrae,

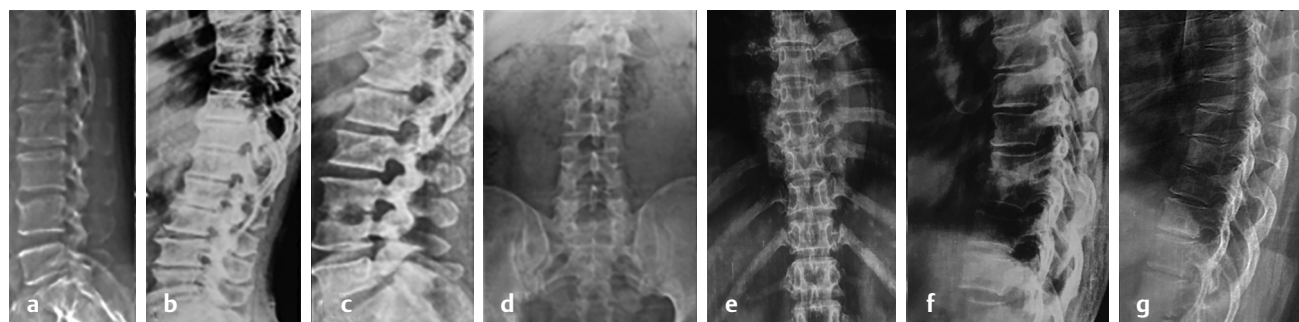


Fig. 2.2 (a) Involvement of the anterior margin of the vertebral body adjacent to the end plates. (b) Para-diskal haziness and disk space narrowing. (c) Marked erosion of adjacent end plates with marked disk space narrowing. (d) Marked adjacent soft tissue shadow suggestive of psoas swelling. (e, f) Clear disk space narrowing due to its destruction. (g) Osteoporosis and lysis of the vertebral body.



Fig. 2.3 Radiograph showing T6–T7 intervertebral disk space narrowing and paravertebral abscess as a fusiform radio-dense shadow called “the bird nest appearance.”

concavities, and scalloping (“*aneurysmal* phenomenon”) on the anterior margin of the vertebral body due to the mass effect,¹³ “Gouge defect,” erosions in the lateral and anterior margin due to a subperiosteal lesion under the anterior longitudinal ligament,¹⁴ and new bone formation are evident in later stages. Cold abscesses are identified as adjacent soft tissue shadows specific to the region involved with characteristic calcifications.

CT scan

The high resolution and tomographic nature of CT scan helps for better identification of the lesion.¹⁴ The characteristic features of spinal TB are anterior vertebral body destruction and collapse, narrowing of disk space, and paravertebral abscesses with calcifications (**Fig. 2.4a, b**). There are four patterns of bone destruction noticed: fragmentary, subperiosteal, osteolytic, and well-defined, localized sclerotic margins.¹⁶ Although anterior column involvement is common, isolated posterior elements involvement is seen (**Fig. 2.4c**). Osteolytic lesions in the pedicle, lamina, spinous process, and transverse process get well identified on axial sections. Presence of aneurysmal pattern, central body involvement of the vertebrae, reactive sclerosis causing ivory vertebrae, isolated



Fig. 2.4 (a) Sagittal section showing clear destruction of the vertebrae adjacent to disk. (b) Coronal section highlighting right-sided tubercular iliopsoas abscess. (c) Sagittal section showing posterior element destruction.

involvement of posterior elements, craniovertebral involvement, and noncontiguous vertebral involvement constitute the features of atypical presentations better appreciated on CT.¹⁷ The greatest value of CT arises during the assessment of spinal canal encroachment due to extension of inflammatory material with bony pieces in the late stage facet arthritis and mechanical bony stenosis. Prompt evaluation of “spine at risk”¹⁸ radiological signs in pediatric spinal TB like separation of the facet joint, retropulsion, lateral translation, and toppling can be made due to its better delineation of facet joints.

Does it have value in diagnosis?

CT scan has higher precision in early identification and obtaining comprehensive information regarding the status of diseased bone, tubercular abscesses, collapse, stability of segment, and spinal canal dimensions. Although it detects destruction before the collapse, it cannot detect the earliest subchondral marrow and end plate changes. CT-guided tissue sampling reduces error in sample acquirement.

Indications

- Normal-looking radiograph with acute/chronic back pain and systemic features of infection.
- Suspicious disk space narrowing.
- Osteolysis in the posterior elements.
- Assessment of deformity associated with collapse and possibility of instrumentation.
- Identification of bone fragments in the spinal canal and sequestrum.

- Evaluation of craniovertebral and cervicothoracic area lesions.
- CT-guided tissue sampling.

Importance in junction area lesion (craniovertebral and cervicothoracic)

Compound regional anatomy of junctional areas with surrounding vital structures may act as an obstacle to detailed visualization. It evaluates early destruction in spite of the obscurity. Mere information about vertebral destruction is not enough to plan the scheme of management (**Fig. 2.5**). The degree of instability and extent of abscesses should also be known. Three stages of craniovertebral tuberculous spondylitis^{19,20} have been described on CT images:

1. Minimal bone destruction without disruption of atlanto-axial joint.
2. Atlanto-axial subluxation and proximal translocation of odontoid process.
3. Extensive bone involvement with destruction of odontoid process and anterior arch of the atlas, resulting in atlanto-axial dislocation.

Pediatric spinal lesions affect multiple vertebral levels which may result in severe kyphotic deformities termed as “Buckling collapse”⁴ which is better evaluated on CT.

Importance in deciding the treatment

CT imaging helps in diagnosis and decision-making regarding reconstruction. CT-guided biopsy from the diseased tissue improves the diagnostic accuracy.²¹ Therapeutic aspiration of a large cold abscess helps in



Fig. 2.5 Complex regional anatomy of cervicothoracic junction making evaluation of the disease process difficult on plain radiographs.

drainage in spite of positional difficulties of the patient.²² CT provides knowledge about the amount of destruction, and a key role of CT-guided intraoperative navigation is to perform instrumentation by clear delineation of the compound anatomy.²³ For patients displaying symptoms of cord compression and regional kyphosis, a high-resolution CT scan plays a crucial role in identifying the specific nature of the material responsible for the cord compression, such as an abscess, bony ridge, or necrotic bone. In cases of laminectomy defects where the feasibility of posterior bone grafting is limited, a CT scan provides valuable information for enhancing the precision of planning the reconstruction of the anterior column.²⁴

Spinal tuberculosis magnetic resonance imaging (MRI)

MRI is the most sensitive of all diagnostic investigations for spinal infections.²⁵ MRI has the advantage of improved contrast resolution for bone and soft tissues along with the versatility of direct imaging in multiple planes.²⁶

Spinal TB lesion in different MRI sequences

The routine MRI sequences acquired are T1-weighted (T1W) and T2-weighted (T2W) sagittal and axial sequences along with sagittal short tau inversion recovery (STIR) sequences. Coronal sequences are acquired to delineate extent of paravertebral and cold abscesses. STIR sequences differentiate fluid from fatty components. The delineation of abscess wall, meningeal inflammation, disk abscess, and intraosseous abscess is better appreciated on Gd-DTPA contrast-enhanced MRI.²⁷

The appearance of various lesions on MRI is detailed in **Table 2.2** and **Fig. 2.6**. Both paravertebral abscess and epidural abscess appear as soft tissue collection with peripheral rim enhancement on postcontrast sequences.²⁸

Arachnoiditis appears as enhancement of dura in postcontrast images with clumping of nerve roots. Thickening of the dura–arachnoid complex appears as an enhancement of the dura–arachnoid in postcontrast images.²⁹ Intradural abscess appears hypointense in T1W and hyperintense in T2W sequences within the dural sheath. Intramedullary and intradural granuloma appears as a ring-enhancing lesion within the spinal cord and within the dural sheath separate from the substance of the cord, respectively.

Diagnostic accuracy and specificity (specific MRI features of spinal tuberculosis)

MRI has high sensitivity and specificity for disruption of the end plate (100% and 81.4%, respectively), paravertebral soft-tissue shadow (96.8% and 85.3%), and high signal intensity of the intervertebral disk on the T2W sequences (80.6% and 82.4%).³⁰ One of the earliest findings on MRI is end plate edema.³¹ The incidence of marrow edema in spinal TB is almost 100% in T1W and T2W sequences^{32,33,34} (**Table 2.3**).

The preservation of disks despite extensive bone destruction is virtually pathognomonic of spinal TB.³⁵ The lack of proteolytic enzymes in mycobacteria might be responsible for relative sparing of the disk. Disk destruction begins only when adjoining vertebral bodies

Table 2.2 MRI signal intensities of various spinal tuberculosis lesions in different sequences

Lesion	T1-weighted	T2-weighted
Bone marrow edema	Hypointense	Hyperintense/Isointense
Diskitis	Hypointense	Hyperintense
Epidural abscess	Hypointense	Hyperintense
Paravertebral abscess	Hypointense	Hyperintense
Cord edema	Hypointense in the substance of cord	Hyperintense in the substance of cord
Myelomalacia	Focal area of hypointense	Focal area of hyperintense

Abbreviation: MRI, magnetic resonance imaging.

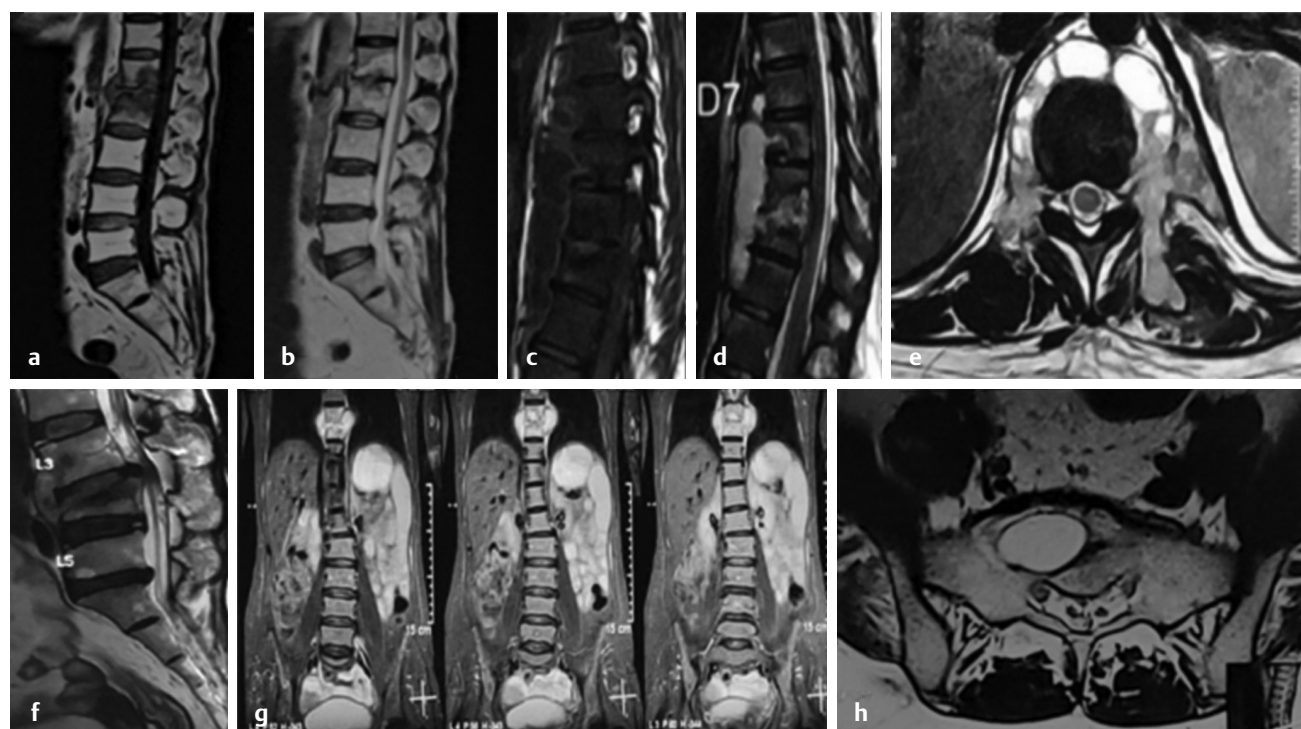


Fig. 2.6 Spinal tuberculosis lesions in various sequences. **(a, b)** T1-weighted and T2-weighted images showing marrow edema as hypointense and hyperintense lesions, respectively, along with end plate erosions. **(c–e)** Short tau inversion recovery (STIR) images showing the subligamentous spread of abscess in sagittal and axial sections. **(f)** Paradiskal lesions with preserved disk space pathognomonic of spinal tuberculosis. **(g)** Coronal section depicting the extent of paravertebral abscess as hyperintense lesions in T2-weighted images. **(h)** Intraosseous abscess appearing as hyperintense lesions in the T2-weighted image.

Table 2.3 Comparison of MRI features of tuberculous and pyogenic spondylodiskitis

Variable	Tuberculosis	Pyogenic
Vertebral body enhancement pattern	Heterogeneous and focal	Homogenous
Number of vertebrae involved	Multiple	Less than two
Disk status	Relatively preserved	Disk destruction
Paravertebral abscess	Present	Absent
Abscess wall	Thin and smooth	Thick and irregular
Skip lesions	Seen occasionally	Absent
Subligamentous spread	Present	Absent

Abbreviation: MRI, magnetic resonance imaging.

are structurally weakened. Various studies showed incidence of paravertebral abscess and epidural abscesses is between 58– and 100% and 53.3 and 85.7%, respectively. The accuracy of MRI in distinguishing granulation tissue

from cold abscess has increased with the advent of post-contrast imaging.³⁶ One of the greatest limitations of MRI is its inability to identify soft tissue calcification on normal scans.

Classical features of marrow edema, paravertebral collection, end plate erosion, and subligamentous spread appear in combination on MRI in TB of spine (**Fig. 2.7**). The presence of single vertebral lesions, isolated posterior element's involvement, and circumferential involvement on MRI are atypical features.³⁷

Resolution of marrow edema, paravertebral abscess, and replacement of marrow with fat are characteristic findings of healing disease.²⁹

PET scan

Positron emission tomography/CT scan has an advantage of associating microbiological, immunological, and pharmacological aspects of TB with anatomic information thus allowing holistic approach in the management.³⁸ Nuclear imaging by ¹⁸F-fluorodeoxyglucose (18F-FDG) is used to assess disease activity, determine extent of disease, and detect the granulomas.^{39,40,41} The principle lies in the accumulation of tracer in the inflammatory cells such as activated macrophages and neutrophils at the lesions.⁴² Active disease avidly receives tracer and can be useful to investigate degree of activity. Multilevel vertebral involvement will depict a "Pine tree" appearance (**Fig. 2.8**).⁴³ Being a nonspecific tracer, 18F-FDG may not differentiate tubercular infection from neoplasms and other conditions.⁴⁴ Antitubercular drugs are also labelled with radioisotopes to evaluate the pharmacokinetics and biodistribution,⁴⁵ and to aid in prognostication of the disease on usage of anti-tuberculosis treatment (ATT).⁴⁶ Higher standard uptake levels of the tracer on FDG-PET are seen in tuberculous infection when compared with pyogenic etiology.⁴⁷

Laboratory test

An increased total white blood cell (WBC) count with relative lymphocytosis is commonly associated with TB infection. The proinflammatory markers (erythrocyte sedimentation rate [ESR] and C-reactive protein [CRP]), though nonspecific to TB, are commonly evaluated.⁴⁸ TB is usually associated with elevated ESR (>20 mm/hour) in 60 to 83% of the patients, which begins to normalize

when active infection subsides. Persistently elevated markers may indicate poor response to therapy, non-compliance, drug resistance, or wrong diagnosis.

Serological tests assess host immune response to diverse mycobacterium antigens. Mantoux tuberculin skin test is a lymphocyte-based immune response serological test with positivity of about 62 to 90%. A positive test indicates that the individual has been exposed to antigen but may not indicate active infection.

Interferon gamma release assays (IGRAs) (QuantiFERON-TB and QuantiFERON-TB Gold-inTube) are whole blood-based enzyme-linked immunosorbent assay (ELISA) measuring the amount of IFN-g produced in response to *Mycobacterium tuberculosis* antigens. Kumar et al reported that the QuantiFERON assay had an estimated sensitivity and specificity of 84% and 95%.⁴⁸ These tests provide quick and specific results but due to lack of specific antigens and inability to differentiate active and healed disease or natural infection and BCG-induced reaction, these are no longer recommended for diagnosis of active TB.^{49,50}

The lymphocyte-monocyte ratio is increasingly adopted with promising results to monitor the therapeutic response.⁴⁷

Soft tissue evaluation

Clinical features, laboratory parameters, and imaging studies play a major part in diagnosis but biopsy is often needed to confirm the diagnosis.

Biopsy: procedure and approach for specific spinal region

Obtaining adequate and appropriate samples either by open or closed approach from the infected foci is a key step. Open biopsy has about 98% accuracy; however, it is associated with common risks.⁵¹ The overall accuracy of a spine biopsy ranges from 16 to 92%, and the complication rates ranges from 0 to 10%.^{52,53} Percutaneous biopsy is becoming increasingly more common (**Fig. 2.9**).

For vertebral lesions with doubtful diagnosis of TB and at safely approachable locations, radiographic image guided (X-ray) biopsy can be performed. For craniovertebral lesions, cervical spine and concealed areas of thoracic

spine, CT-guided biopsy should be considered to get adequate amount of sample safely. In patient with spinal TB requiring surgical management in view of debilitating deformity or progressive neurological deficits, open biopsy should be considered simultaneously (**Fig. 2.10**).

Approaches

Posterior or direct approach is commonly used in all regions of spine.⁵⁴ For transpedicular approach, the patient is placed in prone position and under fluoroscopy the level of the involved segment is marked. Following standard aseptic precautions, under local infiltration, stab incision is made, and Jamshidi needle is inserted and pushed inside till the pedicle. Care is taken that the medial and inferior wall of the pedicle is not breached. Once the position is confirmed, the trochar needle is removed, and trochar is driven inside by screwing movements till the desired spot of lesion is reached, after which by making sequential rotatory movements trochar is extracted.

Safe approach varies with the region of the spine involved (**Table 2.4**).

Cervical spine

- C1–C3: Transoral approach is used in approaching pathology involving cervicomedullary junction where direct decompression is achieved. Patient is placed in supine position under nasotracheal intubation, with a transoral retractor to keep the jaws

wide open, C1 tubercle is palpated over the posterior pharyngeal wall, and incision is made mid-line centering C1 tubercle.

- C2–C7: Anterolateral approach is commonly used. Under image guidance, the needle passed in between the airway and the carotid artery while pushing the contents of the carotid sheath away from the tip of the needle. Care should be taken that the needle is directed medially and superiorly while approaching C2–C3 lesions and for lesions in C1 lateral mass.
- C4–C7: Posterolateral approach has been described for C4 to C7 vertebral lesions. The needle is advanced between the posterior edge of the sternocleidomastoid muscle and the vertical line traced from the tip of mastoid.

Thoracic and lumbar spine

Refer **Table 2.4**.

Sacrum

Sacral lesions can be approached either by posterior or posterolateral approach.

Open biopsy tissue sampling is done simultaneously with the surgical procedure.

Increasing the specimen accuracy: CT-guided biopsy increases accuracy with adequacy and accuracy of about 92.6 and 90.2%.⁵⁴

Table 2.4 Other commonly used approaches for thoracic and lumbar spine

Approach	Specific region	Position	Plane	Considerations
Posterolateral	Thoracic and lumbar	Prone/decubitus	The needle is introduced lateral to the transverse process (5–7 cm from the midline) and the tip is aimed at the lateral side of the vertebral body	Thoracic from right side to prevent damage to aorta and lumbar from left side to protect IVC
Transcostovertebral	Thoracic	Prone or lateral position	Between the anterior aspect of transverse process and the posterior part of the rib neck and then it is directed through the costovertebral joint to the lesion	Avoids the risk of pleural puncture
Transforminodiscal	Thoracic and lumbar	Prone	Superior concave surface of the vertebra is the entry point of the needle	Superomedial part of the vertebra cannot be accessed

Abbreviation: IVC, inferior vena cava.



Fig. 2.7 Para-diskal lesion in thoracic spine with marrow edema, end plate erosion, epidural abscess, subligamentous abscess spread, and reduction of vertebral height are characteristic of spinal tuberculosis.

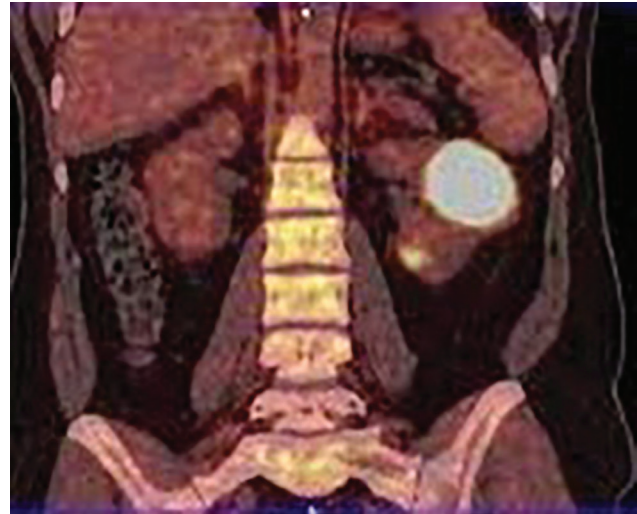


Fig. 2.8 “Pine tree” appearance on positron emission tomography–computed tomography (PET-CT) scan due to tracer uptake by infective tissue.

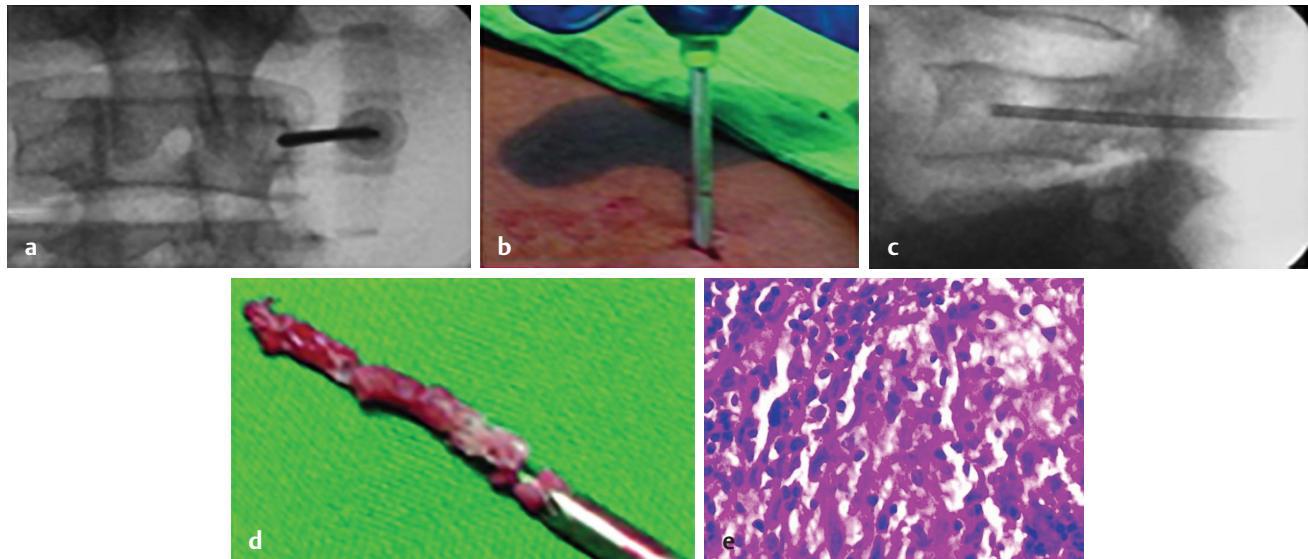


Fig. 2.9 Illustration showing the technique of transpedicular biopsy. **(a)** The entry point was made under image intensifier in anteroposterior view. **(b)** A small stab incision was made and the Jamshidi biopsy needle was introduced into the pedicle. **(c)** The stylet was removed, and trocar was advanced into the pedicle by rotatory movements under image intensifier in lateral view. **(d)** The harvested biopsy material. **(e)** Histopathological examination showing epithelioid cells, foamy macrophages, and lymphocytes along with Langhans giant cells and foreign body giant cells.

Intraoperative scrape cytology is a rapid and inexpensive technique useful in obtaining 100% diagnostic yield.⁵⁵ Acquired sample is screened intraoperatively by rapid smearing with H&E stain. It takes around 8–10 minutes for interpretation of results. Based on results if sample is adequate rest of the tissue is sent for evaluation; repeat samples are obtained if smear is inconclusive or sample is inadequate.

Tissue-specific diagnostic test

Tissue-specific diagnostic tests include demonstrating bacilli in microscopy, isolating bacteria from cultures, and molecular studies.

- Ziehl-Neelsen (ZN): ZN microscopy is a routinely used technique which is simple, cost effective, and rapid. Sensitivity of ZN staining for pulmonary TB was reported to be about 25–75%.⁵⁶ It requires presence of at least about 10^4 to 10^5 bacilli/mL in the specimen for the test to be positive. Osseous lesions being paucibacillary, staining of osseous samples is unlikely to show any bacillus.⁵⁷
- Bacterial culture and drug sensitivity tests: Most common solid medium used for cultures is Löwenstein-Jensen (LJ) medium with a positive detection rate ranging from 0 to 75%.⁵⁸ Cultures may take 4 to 6 weeks for obtaining results. The Agar environment (BACTEC) is the current standard medium, and it allows for early assessment of drug susceptibility. BACTEC and LJ media had positivity rates of 83.87 and 61.29%, respectively, with the average detection time being 11.3 and 26.7 days.⁵⁹
- Cartridge based nucleic acid amplification test (CBNAAT): Xpert MTB/RIF test detects DNA sequences specific for *Mycobacterium tuberculosis* and rifampicin (RPM) resistance by means of polymerase chain reaction.⁴⁸ Steingart et al showed that this test was highly accurate, with sensitivity and specificity of 88% and 98%.^{59,60} The test is so rapid that it takes around 90 minutes for obtaining results and is particularly useful in cases with low bacilli load, as few as 10–50 bacilli.

- Line probe assay technology: It is based on reverse hybridization of DNA on the strip. This is a rapid test used to detect *Mycobacterium tuberculosis* complex (MTB) as well as drug sensitivity to RPM and isoniazid (INH) due to mutations in the *inhA* and *katG* genes, while the Xpert MTB/RIF can detect only RPM resistance. Delay in diagnosis of spinal TB is well known with an average mean delay of 6–8 months before the diagnosis is made. There is further delay of a minimum of 5–6 months for diagnosing drug-resistant spinal TB, only after the patient shows no response to the treatment.

In 2008, WHO endorsed GenoTypeMTBDRplus (version 1.0) molecular line probe assay (LPA), which is a rapid detection procedure of MTB and serves to detect mutations in the resistance-specific genes conferring resistance against Rifampicin (RIF) and Isoniazid (INH) in acid-fast bacilli (AFB) smear-positive sputum specimens. Use of LPA has shown direct benefits for both the patient and community. In their study, Xu lan et al and Li L et al reported a mean delay of 8.52 +/- 6.15 months and 8.25 +/- 2.76 months, respectively, in making diagnosis of drug-resistant spinal TB.⁶¹ Multiple other studies have recommended that drug sensitivity testing should be carried out on all initial and re-treatment cases of spinal TB.

Histopathological examination reveals typical findings like large caseating necrotizing granulomas with epithelioid and multinucleated giant cells with lymphocytic infiltration (**Fig. 2.11**). The histology is diagnostic in 60% of cases.⁶² Mateo et al⁵⁷ in their study found that 62.3% had positive histological evidence with the most common findings of multinucleated and Langhans giant cells (56%) and epithelioid granuloma (70%).⁶³

Differential diagnosis of spinal TB (TB is a great mimic)

There are many conditions mimicking TB.⁶⁴ However, final diagnosis is made in cases of doubtful diagnosis by tissue evaluation. Gross mimics of spinal TB can be grouped based on their clinical or radiological or histopathological resemblance (**Table 2.5**).

Table 2.5 Clinical, radiological, and histopathological mimics

Clinical mimics	Radiological mimics	Histopathological mimics
Pyogenic spondylitis	Early trauma	Histiocytosis X
Brucellosis	Metastasis	Sarcoidosis
Postoperative diskitis	Primary tumors	Mycotic infections
Syphilis	Ankylosing spondylitis	Syphilis
Typhoid	Osteoporotic fractures	Blastomycosis
Mycotic diskitis	Lymphoma	Histoplasmosis
	Multiple myeloma	

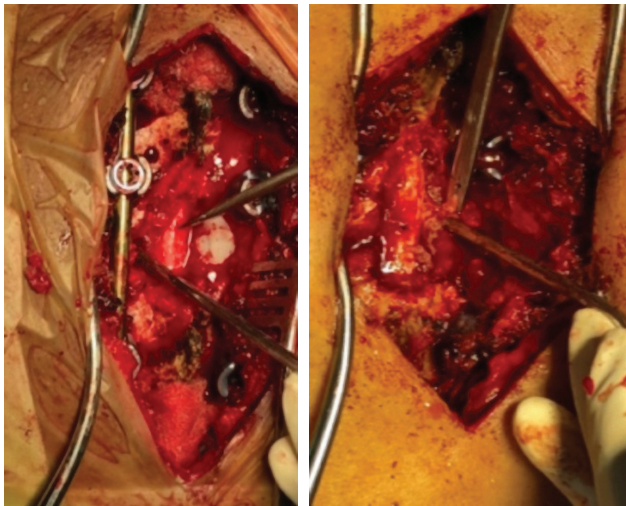


Fig. 2.10 Intraoperative images showing disk material and granulation tissue samples collected during surgical fixation.

Clinical and radiological differences (Table 2.6)

Spinal TB is one of the commonest extrapulmonary sites for TB. Being a deep-seated paucibacillary lesion, diagnosis is often delayed. Clinically, spinal TB mimics various other common conditions which may influence the process of diagnosis and adequate management.

It is important to know the various modes of presentations and different diagnostic tools to avoid erroneous management.

Laboratory investigations like complete blood picture, ESR, and CRP help in monitoring the activity of disease and response to the treatment. Bacteriological and histological evaluation helps in making diagnosis of spinal TB. Demonstration of AFB is possible in about 10–30% of cases. Conventional culture is the gold standard for both bacteriological and drug sensitivity testing. However, turnaround time of 2–6 weeks for detection and additional 3 weeks for drug sensitivity testing (DST) is major limitation. To shorten the delay rapid culture techniques have been introduced like BACTEC and GeneXpert MTB/RIF which have shortened the time required for diagnosis and are specific. However, assessment of drug resistance has been a common issue faced in a country like India where the prevalence of spinal TB is high. To overcome the delay in detecting the multidrug and extended drug resistance, many studies have recommended use of LPA along with the standard techniques for earlier detection of drug sensitivity and formulating an appropriate treatment regimen.

Table 2.6 Diagnosis, site of predilection, clinical features, radiological features, and characteristic features

Diagnosis	Typical site of predilection	Clinical features	Radiological features	Characteristic features
Pyogenic spondylitis ⁶⁴	Lumbar and cervical region	High grade persistent fever, severe pain, rapid progression, myelopathy	Destruction of vertebral bodies < disk spaces, sclerosis, homogenous marked enhancement, small paravertebral lesion and epidural extension, thick and irregular abscess	Rapid disk destruction, sparing of posterior elements
Brucellar spondylitis ⁶⁵	Lumbar spine	Fever, malaise, weight loss, back pain, myelopathy	Intact architecture, lytic lesions in disko-vertebral junction, sclerosis, small paraspinous lesion anterior osteophytes	Anterior parrot beak, gas in the disks, sparing of posterior elements, history of ingestion of unpasteurized milk or contact with goats
Typhoid spine ⁶⁶	Lumbar spine	History of enteric fever, excruciating pain and muscle spasm	Resembles to that of tuberculosis and low-grade pyogenic spondylitis	Rarity of disease, vertebral osteomyelitis, specific agglutination tests
Mycotic spondylitis ⁶⁷	Nonspecific	Back pain, radicular irritation syndrome, in rare cases various degrees of neurological deficit	Generally nonspecific, relative sparing of the disk, absence of T2-hyperintense band in the disk, absence of postcontrast disk enhancement, blastomycosis—paravertebral abscesses, actinomycosis—sclerosis and bone destruction	Honeycomb or lattice like appearance of vertebrae, multiple sinus formation, involvement of subcutaneous tissue, confirmation only by demonstration of mycotic organisms
Ankylosing spondylitis ⁶⁸	SI joints, axial skeleton	Dull pain in gluteal and lumbar region, morning stiffness, reduced chest expansion, kyphotic deformity, severe restriction of movements	Sacroiliitis, synovial enhancement, enthesitis, ossification of ligaments, AF, and disk	Bamboo spine, dagger sign, Romanus lesion, Andersson lesion, vertebral body squaring enthesophytes, pseudoarthrosis
Rheumatoid arthritis ⁶⁹	Cervical spine	Polyarthralgia, morning stiffness, late-onset neck pain, instability and neurological symptoms	Bone erosions, atlantoaxial subluxation, bone marrow edema, synovitis, narrowing of the spinal canal	Arthritic changes in other peripheral joints, presence of extradural pannus tissue
Lymphoma ⁷⁰	Skip or contiguous multilevel involvement	Malaise, backache, fever	Lytic lesions, paraspinal masses, epidural lesions	Paraspinal masses with vertebral lesion but no extensive cortical bone destruction
Metastases ⁷¹	Thoracic spine	Bone pain at night, back pain, myelopathy, presence of systemic malignancy	Lytic or sclerotic lesions, bony destruction with epidural mass	Vertebral body and posterior elements lesions, preserved disks, halo sign

(Continued)

Table 2.6 (Continued) Diagnosis, site of predilection, clinical features, radiological features, and characteristic features

Diagnosis	Typical site of predilection	Clinical features	Radiological features	Characteristic features
Multiple myeloma ⁷²	Multilevel involvement	Pain, permanent deformity, kyphosis, walking impairment, permanent disability, paralysis	Predilection to vertebral body, more rare in transverse process and posterior elements, vertebral collapse, end plate lesions, vertebral wedge lesions	Multiple punched-out lesions of skull, Bence Jones proteins, M band in immunoelectrophoresis, myeloma cells in biopsy
GCT ⁷³	GCT: sacrum	Pain, diurnal variation, neurological symptoms, pathological fractures	Usually involves vertebral bodies, osteolytic expansile eccentric growth, late involvement of disk spaces	Mostly one segment, moth eaten radiolucent erosive lesion
Modic changes ⁷⁴	Lumbar spine	Chronic pain, radiculopathy, myelopathy, scoliosis	Disk degeneration, Modic changes especially Type 1, end plate changes, maintained vertebral body height	Single or multiple segment involvement, no sudden neurological deterioration, elderly age groups, absence of constitutional symptoms

Abbreviations: AF, annulus fibrosus; GCT, giant cell tumor; SI, sacroiliac.

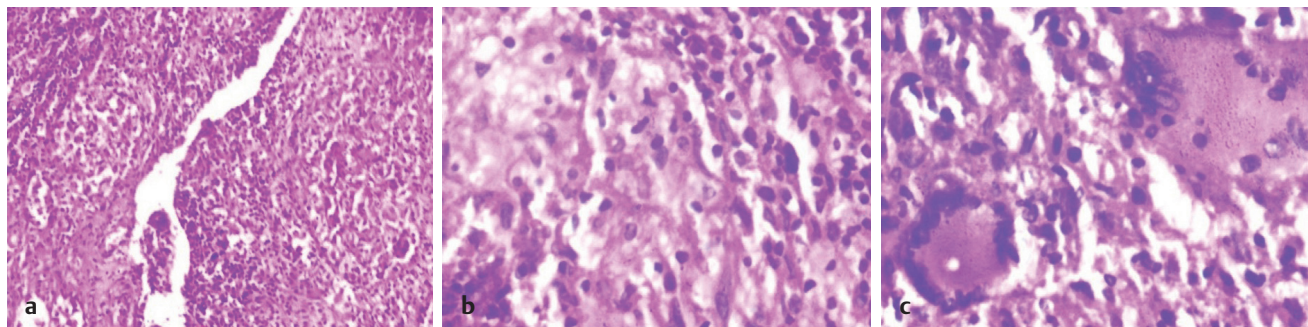


Fig. 2.11 Histopathological examination revealing typical (a) epithelioid cells, (b) foamy macrophages, lymphocytes, and (c) foreign body and Langhans giant cells.

Key points

- Multidisciplinary approach: Diagnosis of tuberculous spondylodiskitis requires a multidisciplinary approach involving the treating surgeons, infectious disease specialists, radiologists, and pathologists. Communication among these specialties is important to obtain accurate diagnosis, initiate appropriate treatment, and monitor the patient's response to chemotherapy.
- High clinical suspicion: Because of the nonspecific nature of symptoms and variable presentation, it is important to maintain a high level of suspicion for TB. Particular attention should be paid to risk factors such as previous history of TB and immunodeficiency.
- Radiological evaluation: Imaging plays an important role in the diagnosis of tuberculous spondylodiskitis. A combination of plain radiographs, CT, and MRI helps to identify characteristic features such as vertebral body destruction, disk space narrowing, and paraspinal abscesses.
- Confirmatory microbiological evidence: Obtaining microbiological evidence is essential for an accurate diagnosis. A combination of diagnostic tests including AFB smears, mycobacterial cultures, and nucleic acid amplification tests (NAATs) should be used. Biopsy of the affected tissue or fluid collection is often necessary to isolate the causative organism and determine drug susceptibility.

References

1. Rajasekaran S. Natural history of Pott's kyphosis. *Eur Spine J* 2013;22(Suppl 4):634–640
2. Rajasekaran S, Kanna RM, Shetty AP. Pathophysiology and treatment of spinal tuberculosis. *JBJS Rev* 2014;2(9):1–13
3. Jain AK, Kumar J. Tuberculosis of spine: neurological deficit. *Eur Spine J* 2013;22(Suppl 4):624–633
4. Subramani S, Shetty AP, Kanna RM, Shanmuganathan R. Ossified ligamentum flavum causing neurological deficit above the level of post-tuberculous kyphotic deformity. *J Clin Orthop Trauma* 2017;8(2):174–177
5. Hodgson AR, Skinsnes OK, Leong CY. The pathogenesis of Pott's paraplegia. *J Bone Joint Surg Am* 1967;49(6):1147–1156
6. Bhargava SK, Gupta S. Large retropharyngeal cold abscess in an adult with respiratory distress. *J Laryngol Otol* 1990;104(2):157–158
7. Shetty AP, Viswanathan VK, Rajasekaran S. Cervical spine TB—current concepts in management. *J Orthop Surg (Hong Kong)* 2021;29(1 suppl):23094990211006936
8. Faure E, Souilamas R, Riquet M, et al. Cold abscess of the chest wall: a surgical entity? *Ann Thorac Surg* 1998;66(4):1174–1178
9. Mallick IH, Thoufeeq MH, Rajendran TP. Iliopsoas abscesses. *Postgrad Med J* 2004;80(946):459–462
10. Oniankitan O, Fiany E, Kakpovi K, Agoda-Koussema LK, Mijiyawa M. Sacrum Pott's disease: a rare location of spine tuberculosis. *Egypt Rheumatol* 2014;36(4):209–211
11. Lindahl S, Nyman RS, Brismar J, Hugosson C, Lundstedt C. Imaging of tuberculosis. IV. Spinal manifestations in 63 patients. *Acta Radiol* 1996;37(4):506–511
12. Shanley DJ. Tuberculosis of the spine: imaging features. *AJR Am J Roentgenol* 1995;164(3):659–664
13. Chapman M, Murray RO, Stoker DJ. Tuberculosis of the bones and joints. *Semin Roentgenol* 1979;14(4):266–282
14. Rivas-Garcia A, Sarria-Estrada S, Torrents-Odin C, Casas-Gomila L, Franquet E. Imaging findings of Pott's disease. *Eur Spine J* 2013;22(Suppl 4):567–578
15. Hodgson AR, Wong W, Yau A. X-ray appearance of tuberculosis of the spine. Springfield, IL: Charles C Thomas; 1969
16. Jain R, Sawhney S, Berry M. Computed tomography of vertebral tuberculosis: patterns of bone destruction. *Clin Radiol* 1993;47(3):196–199
17. Yalniz E, Pekindil G, Aktas S. Atypical tuberculosis of the spine. *Yonsei Med J* 2000;41(5):657–661

18. Rajasekaran S. Kyphotic deformity in spinal tuberculosis and its management. *Int Orthop* 2012;36(2):359–365
19. Lifeso R. Atlanto-axial tuberculosis in adults. *J Bone Joint Surg Br* 1987;69(2):183–187
20. Megaloikononimos PD, Igoumenou V, Antoniadou T, Mavrogenis AF, Soultanis K. Tuberculous spondylitis of the craniovertebral junction. *J Bone Jt Infect* 2016;1:31–33
21. Gul SB, Polat AV, Bekci T, Selcuk MB. Accuracy of percutaneous CT-guided spine biopsy and determinants of biopsy success. *J Belg Soc Radiol* 2016;100(1):62
22. Hayashi N, Takeuchi Y, Morishita H, Ehara N, Yamada K. CT-guided femoral approach for psoas muscle abscess drainage. *Cardiovasc Intervent Radiol* 2022;45(4):522–526
23. Baky FJ, Milbrandt T, Echternacht S, Stans AA, Shaughnessy WJ, Larson AN. Intraoperative computed tomography-guided navigation for pediatric spine patients reduced return to operating room for screw malposition compared with freehand/fluoroscopic techniques. *Spine Deform* 2019;7(4):577–581
24. Tang Y, Wu WJ, Yang S, et al. Surgical treatment of thoracolumbar spinal tuberculosis—a multicentre, retrospective, case-control study. *J Orthop Surg Res* 2019;14(1):233
25. Jain AK. Tuberculosis of the spine: a fresh look at an old disease. *J Bone Joint Surg Br* 2010;92(7):905–913
26. Ansari S, Amanullah MF, Ahmad K, Rauniyar RK. Pott's spine: diagnostic imaging modalities and technology advancements. *N Am J Med Sci* 2013;5(7):404–411
27. Maurya VK, Sharma P, Ravikumar R, et al. Tubercular spondylitis: a review of MRI findings in 80 cases. *Med J Armed Forces India* 2018;74(1):11–17
28. Jain AK, Sreenivasan R, Saini NS, Kumar S, Jain S, Dhammi IK. Magnetic resonance evaluation of tubercular lesion in spine. *Int Orthop* 2012;36(2):261–269
29. Danchaijitr N, Temram S, Thepmongkhon K, Chiewvit P. Diagnostic accuracy of MR imaging in tuberculous spondylitis. *J Med Assoc Thai* 2007;90(8):1581–1589
30. Currie S, Galea-Soler S, Barron D, Chandramohan M, Groves C. MRI characteristics of tuberculous spondylitis. *Clin Radiol* 2011;66(8):778–787
31. Chang MC, Wu HT, Lee CH, Liu CL, Chen TH. Tuberculous spondylitis and pyogenic spondylitis: comparative magnetic resonance imaging features. *Spine* 2006;31(7):782–788
32. Akman S, Sirvanci M, Talu U, Gogus A, Hamzaoglu A. Magnetic resonance imaging of tuberculous spondylitis. *Orthopedics* 2003;26(1):69–73
33. Yusof MI, Hassan E, Rahmat N, Yunus R. Spinal tuberculosis: the association between pedicle involvement and anterior column damage and kyphotic deformity. *Spine* 2009;34(7):713–717
34. Joseffer SS, Cooper PR. Modern imaging of spinal tuberculosis. *J Neurosurg Spine* 2005;2(2):145–150
35. Kotze DJ, Erasmus LJ. MRI findings in proven Mycobacterium tuberculosis (TB) spondylitis. *SA J Radiol* 2006;10(2):6–12
36. Pande KC, Babhulkar SS. Atypical spinal tuberculosis. *Clin Orthop Relat Res* 2002; (398):67–74
37. Johnson DH, Via LE, Kim P, et al. Nuclear imaging: a powerful novel approach for tuberculosis. *Nucl Med Biol* 2014;41(10):777–784
38. Ichiya Y, Kuwabara Y, Sasaki M, et al. FDG-PET in infectious lesions: the detection and assessment of lesion activity. *Ann Nucl Med* 1996;10(2):185–191
39. Goo JM, Im JG, Do KH, et al. Pulmonary tuberculoma evaluated by means of FDG PET: findings in 10 cases. *Radiology* 2000;216(1):117–121
40. Sathekge M, Maes A, Kgomo M, Stoltz A, Pottel H, Van de Wiele C. Impact of FDG PET on the management of TBC treatment. A pilot study. *Nucl Med (Stuttg)* 2010;49(1):35–40
41. Vorster M, Sathekge MM, Bomanji J. Advances in imaging of tuberculosis: the role of ¹⁸F-FDG PET and PET/CT. *Curr Opin Pulm Med* 2014;20(3):287–293
42. Kumar Jain T, Sood A, Kumar Basher R, Bhattacharya A, Rai Mittal B, Aggarwal AK. “Pine tree” appearance on ¹⁸F-FDG PET/CT MIP image in spinal tuberculosis. *Rev Esp Med Nucl Imagen Mol* 2017;36(2):122–123
43. Ankrah AO, van der Werf TS, de Vries EF, Dierckx RA, Sathekge MM, Glaudemans AW. PET/CT imaging of Mycobacterium tuberculosis infection. *Clin Transl Imaging* 2016;4:131–144
44. Heysell SK, Thomas TA, Sifri CD, Rehm PK, Houpt ER. ¹⁸F-Fluorodeoxyglucose positron emission tomography for tuberculosis diagnosis and management: a case series. *BMC Pulm Med* 2013;13:14

45. Bassetti M, Merelli M, Di Gregorio F, et al. Higher fluorine-18 fluorodeoxyglucose positron emission tomography (FDG-PET) uptake in tuberculous compared to bacterial spondylodiscitis. *Skeletal Radiol* 2017;46(6):777–783
46. Agarwal A, Bhat MS, Kumar A, Shaharyar A, Mishra M, Yadav R. Lymphocyte/monocyte ratio in osteoarticular tuberculosis in children: a haematological biomarker revisited. *Trop Doct* 2016;46(2):73–77
47. Garg RK, Somvanshi DS. Spinal tuberculosis: a review. *J Spinal Cord Med* 2011;34(5):440–454
48. Kumar R, Das RK, Mahapatra AK. Role of interferon gamma release assay in the diagnosis of Pott disease. *J Neurosurg Spine* 2010;12(5):462–466
49. World Health Organization. Tuberculosis: Serodiagnostic tests policy statement 2011. Accessed March 14, 2014 at: <https://www.who.int/publications/i/item/9789241502054>
50. Mankin HJ, Lange TA, Spanier SS. The hazards of biopsy in patients with malignant primary bone and soft-tissue tumors. *J Bone Joint Surg Am* 1982;64(8):1121–1127
51. Metzger CS, Johnson DW, Donaldson WF III. Percutaneous biopsy in the anterior thoracic spine. *Spine* 1993;18(3):374–378
52. Stringham DR, Hadjipavlou A, Dzioba RB, Lander P. Percutaneous transpedicular biopsy of the spine. *Spine* 1994;19(17):1985–1991
53. Nourbakhsh Ali. Percutaneous spine biopsy: a literature review. *Int J Radiol Radiat Oncol* 2015;1:23–28
54. Naresh-Babu J, Neelima G, Reshma-Begum SK. Increasing the specimen adequacy of transpedicular vertebral body biopsies. Role of intraoperative scrape cytology. *Spine J* 2014;14(10):2320–2325
55. Jain A, Bhargava A, Agarwal SK. A comparative study of two commonly used staining techniques for acid fast bacilli in clinical specimen. *Indian J Tuberc* 2002;49:161–162
56. Kumar M, Kumar R, Srivastva AK, et al. The efficacy of diagnostic battery in Pott's disease: a prospective study. *Indian J Orthop* 2014;48(1):60–66
57. Mateo L, Manzano JR, Olivé A, Manterola JM, Pérez R, Tena X, Prats M. [Osteoarticular tuberculosis. Study of 53 cases] [article in Spanish]. *Med Clin (Barc)* 2007;129(13):506–509
58. Zhou JS, Chen JT, Wu XQ, Jin DD. [Application of BACTEC MGIT 960 system and molecular identification of mycobacteria in the diagnosis of spinal tuberculosis] [article in Chinese]. *J First Mil Med Univ* 2002;22(9):830–832
59. Steingart KR, Sohn H, Schiller I, et al. Xpert® MTB/RIF assay for pulmonary tuberculosis and rifampicin resistance in adults. *Cochrane Database Syst Rev* 2013;1(1):CD009593
60. Boehme CC, Nicol MP, Nabeta P, et al. Feasibility, diagnostic accuracy, and effectiveness of decentralised use of the Xpert MTB/RIF test for diagnosis of tuberculosis and multidrug resistance: a multicentre implementation study. *Lancet* 2011;377(9776):1495–1505
61. Xu L, Jian-Zhong X, Xue-Mei L, Bao-Feng G. Drug susceptibility testing guided treatment for drug-resistant spinal tuberculosis: a retrospective analysis of 19 patients. *Int Surg* 2013;98(2):175–180
62. Allothman A, Memish ZA, Awada A, et al. Tuberculous spondylitis: analysis of 69 cases from Saudi Arabia. *Spine* 2001;26(24):E565–E570
63. Kumaran SP, Thippeswamy PB, Reddy BN, Neelakantan S, Viswamitra S. An institutional review of tuberculosis spine mimics on MR imaging: cases of mistaken identity. *Neurol India* 2019;67(6):1408–1418
64. Lee KY. Comparison of pyogenic spondylitis and tuberculous spondylitis. *Asian Spine J* 2014;8(2):216–223
65. Esteves S, Catarino I, Lopes D, Sousa C. Spinal tuberculosis: rethinking an old disease. *J Spine* 2017;6(1):358–366
66. Khoo HW, Chua YY, Chen JL. Salmonella typhi vertebral osteomyelitis and epidural abscess. *Case Rep Orthop* 2016;2016:6798157
67. Burgetova A, Vaneckova M, Jakubikova M, Prof ZS. Mycotic spondylitis caused by Cladosporium cladosporides: a case report. *J Neurol Res* 2013;3(2):78–80
68. Bron JL, de Vries MK, Snieders MN, van der Horst-Bruinsma IE, van Royen BJ. Discovertebral (Andersson) lesions of the spine in ankylosing spondylitis revisited. *Clin Rheumatol* 2009;28(8):883–892

69. Del Grande M, Del Grande F, Carrino J, Bingham CO III, Louie GH. Cervical spine involvement early in the course of rheumatoid arthritis. *Semin Arthritis Rheum* 2014;43(6):738–744
70. Patnaik S, Jyotsnarani Y, Uppin SG, Susarla R. Imaging features of primary tumors of the spine: a pictorial essay. *Indian J Radiol Imaging* 2016;26(2):279–289
71. Zamzuri Z, Adham SY, Shukrimi A, Azril MA, Amran R. Metastatic adenocarcinoma of the lung mimicking spinal tuberculosis. *Int Med J Malays* 2011;10(2)
72. Tosi P. Diagnosis and treatment of bone disease in multiple myeloma: spotlight on spinal involvement. *Scientifica (Cairo)* 2013;2013:104546
73. Shi LS, Li YQ, Wu WJ, Zhang ZK, Gao F, Latif M. Imaging appearance of giant cell tumour of the spine above the sacrum. *Br J Radiol* 2015;88(1051):20140566
74. Vital JM, Gille O, Pointillart V, et al. Course of Modic 1 six months after lumbar posterior osteosynthesis. *Spine* 2003;28(7):715–720, discussion 721